Science of the Total Environment 738 (2020) 139532

Contents lists available at ScienceDirect

Science of the Total Environment

journal homepage: www.elsevier.com/locate/scitotenv

Characterization of herbaceous encroachment on soil biogeochemical cycling within a coastal marsh

Havalend E. Steinmuller[a], Tammy E. Foster[b], Paul Boudreau[a], C. Ross Hinkle[a], Lisa G. Chambers[a,*]

[a] *Department of Biology, University of Central Florida, 4000 Central Florida Blvd., Orlando, FL 32816, United States of America*
[b] *Kennedy Space Center Ecological Program, IMSS-300, Kennedy Space Center, FL 32899, United States of America*

HIGHLIGHTS

- Soils within encroaching saltgrass and transition zones contain higher soil C and N than in cordgrass zones.
- Both water level and vegetation type mediate enzyme activity and mineralization rates.
- Encroachment accelerates soil C cycling and enhances soil C storage.

GRAPHICAL ABSTRACT

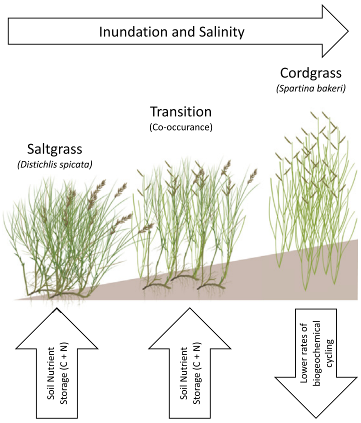

ARTICLE INFO

Article history:
Received 5 November 2019
Received in revised form 12 May 2020
Accepted 16 May 2020
Available online 1 June 2020

Editor: Jay Gan

Keywords:
Sea level rise
Biogeochemical cycling
Distichlis spicata
Spartina bakeri
Encroachment
Herbaceous marsh

ABSTRACT

Vegetation transitions occur globally, altering ecosystem processing of organic matter and changing rates of soil biogeochemical cycling. In coastal marshes, more salt- and inundation-tolerant herbaceous species are encroaching on less tolerant species, concomitant with sea level rise. These species shifts could disrupt ecosystem services such as soil organic matter storage and the cycling of carbon (C), nitrogen (N), and phosphorus (P). To determine how these ecosystem processes were affected by encroachment, we characterized biogeochemical properties and functions along a transect of encroaching *Distichlis spicata* L. *Greene* (saltgrass) on *Spartina bakeri Merr.* (cordgrass), two herbaceous species. During both the wet and dry season, nine soil cores were obtained from three community types: saltgrass end member, transition zone, and cordgrass end member. Total soil C, N, and organic matter were greatest within the saltgrass and transition zones. The saltgrass and transition zone soils also supported higher rates of enzyme activity and potentially mineralizable N and P than cordgrass soils during the dry season, and greater potential CO_2 production and microbial biomass C during the wet season. Generally, the transition zone functioned similarly to the saltgrass zone and the encroachment gradient coincided with a 33 cm elevation change. Seasonally, low extractable nutrient availability (nitrate and soluble reactive phosphorus) during the dry season was correlated with overall greater enzyme activity (*N*-acetyl-β-D-glucosidase, alkaline phosphatase, β-glucosidase, xylosidase, and cellobiosidase) and potentially mineralizable N and phosphorus (P) rates. This study demonstrates that shifts in dominant herbaceous species and accompanying abiotic gradients alters biogeochemical processing of organic matter within coastal marshes.

---

[*] Corresponding author.
E-mail address: lisa.chambers@ucf.edu (L.G. Chambers).

https://doi.org/10.1016/j.scitotenv.2020.139532
0048-9697/

1. Introduction

Shifting abiotic factors associated with climate change are altering the spatial extent of vegetation communities worldwide (Koch and Mooney, 1996; Vitousek et al., 1997). Each plant species occupies a specific zone of tolerance in regards to environmental gradients, such as temperature or salinity, where primary productivity is highest (i.e. Bertness, 1991; Pennings et al., 2004; Pennings and Callaway, 1992). Outside of that optimal zone, plant species are stressed and are uniquely vulnerable to being outcompeted by different vegetation types with more suitable zones of tolerance. Altered global and local climate regimes mediate these vegetation shifts, which have been documented to impact ecosystems through changing regional productivity (Knapp et al., 2008), altering soil nutrient storage (Liao et al. 2008), creating denuded interspaces of bare soil (Darrouzet-Nardi et al., 2006), decreasing regional biodiversity (Ratajczak et al., 2012), and modifying the edaphic environment through rhizosphere interactions, seasonal senescence of biomass, and altered root-associated microbiota, each of which can affect biogeochemical cycling (Ehrenfeld, 2003). Within coastal wetlands, vegetation dominance is primary mediated through factors influencing inundation (anaerobic conditions) and salinity (Bertness, 1991; Pennings et al., 2004); shifts in dominant species are often abrupt and catalyzed by minute differences in microtopography and/or climate (Osland et al., 2016). Global sea level rise threatens to disrupt these established vegetation zonations within coastal wetlands, consequently altering biogeochemical cycling within these ecosystems. Despite occupying <0.03% of land area, coastal wetlands sequester roughly 244.7 g carbon m^{-2} y^{-1} (Ouyang and Lee, 2014), retain and cycle nutrients, and perform other vital ecosystem services with the potential to be disrupted through vegetative encroachment associated with sea level rise.

In this study, we characterized both soil nutrient storage (total C, N, P, and organic matter) and biogeochemical activity (enzyme assays associated with the hydrolysis of organic compounds, potential mineralization rates, carbon dioxide production) across a currently shifting herbaceous-to-herbaceous ecotone in a coastal marsh in an effort to understand how biogeochemical processes relate to vegetative encroachment. Specifically, we characterized the transition of *Distichlis spicata* L. *Greene* (saltgrass) encroaching into areas previously occupied by *Spartina bakeri Merr.* (cordgrass) (referred to throughout as the 'herbaceous-herbaceous' transition) within a subtropical coastal marsh during both the wet and the dry season. The transition zone (where both species co-occur) was included in the analysis to determine how rapidly encroachment alters biogeochemical processes. Through meta-analysis, Liao et al. (2008) suggested invading species generally increase nutrient storage; thus, we anticipated that soil nutrients (total C, N, and organic matter content) would be greatest within the saltgrass zone. We also expected that the process of vegetative encroachment would function as a 'biogeochemical hotspot', with the transition zone supporting highest rates of biogeochemical change (i.e. mineralization, enzyme activity, and nutrient availability) due to the greater diversity in microbial substrates caused by the co-occurrence of the two species. Furthermore, we anticipated that the magnitude of these biogeochemical changes would be affected by seasonality, with greater rates of biogeochemical activity present during the dry season as oxygen availability is higher.

Co-incidentally with a change in vegetation type, we anticipated the existence of a gradient of inundation and ambient salinity due to an elevation gradient, which could be viewed as 'low marsh' community encroaching into a previously 'high marsh' community. These abiotic variables could provide a mechanism for herbaceous encroachment while simultaneously contributing to observed differences in

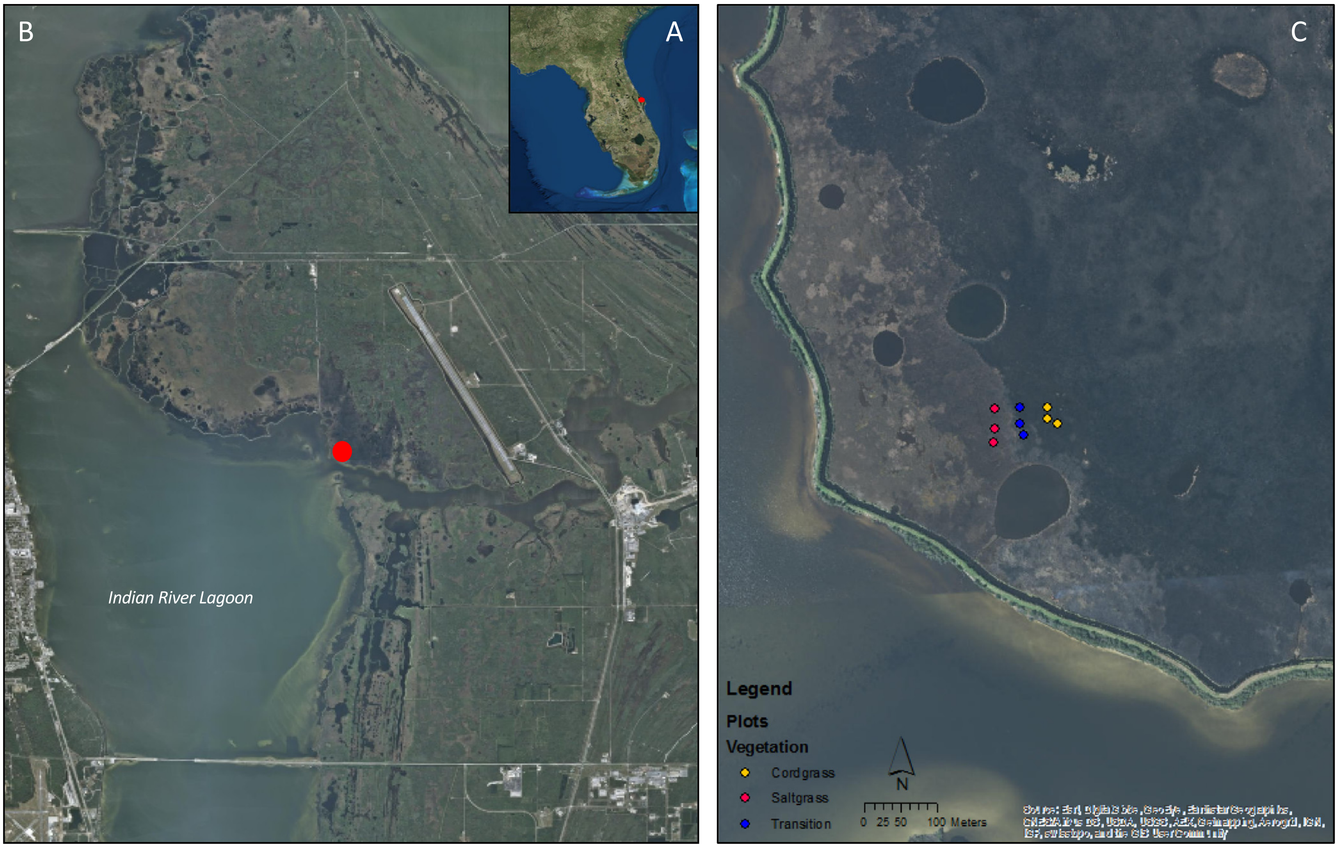

Fig. 1. Location of the study sites within a) the state of Florida, b) Kennedy Space Center/Merritt Island National Wildlife Refuge, and c) within cell T16 as designated by Brevard County Mosquito Control.

biogeochemical characteristics, but such an investigation was not the impetus for this study. Instead, we sought to determine if the 'vegetation transition' (herein referring to both the vegetation shift and accompanying abiotic characteristics) results in altered biogeochemical cycling, with implications for changes in ecosystem services, such as carbon storage, and applications for ecosystem modeling.

2. Methods

2.1. Site description and soil sampling

Three replicate transects were set up within an impoundment at the Merritt Island National Wildlife Refuge, a 567 km^2 area on the eastern coast of Florida, within management cell T-16 (Fig. 1). Each transect consisted of three 2 m^2 plots: one within the saltgrass end member, one within the transition zone (co-occurrence of both species), and one within the cordgrass end member (Fig. 1) for a total of 9 plots. Transects were spaced approximately 10 m apart. Historical aerial imagery (Fig. 2) shows the roughly 60 m change in the leading edge of the transition zone between 1991 and 2014 (Google Earth).

Soils at the site are within the Riomar/Turnbull series: fine, smectitic, nonacid hyperthermic Typic Hydraquents (US Soil Survey 2018). Though historically surrounded by an earthern dike (since the late 1950s – early 1960s; Steward et al., 2003), Hurricane Irma (2017) destroyed the dikes around this wetland prior to the first sampling, effectively hydrologically connecting the site with the adjacent Indian River Lagoon (IRL). A 251 km long lagoon, the IRL is microtidal, with salinity between 29 and 40 ppt (USGS Monitoring Station at Haulover Canal). Water levels at the site are regulated by the combination of tidal forcings, precipitation, and wind energy related to seasonality. Wet season occurs during the late summer and fall of each year, while the dry season occurs between the late winter and early spring (Foster et al., 2017). Water level and salinity at the site were recorded from August 2017 to February 2018 with U20 water level logger (Onset, Bourne, MA, USA) and a U24 high-salinity conductivity logger (Onset, Bourne, MA, USA), each deployed in a well (PVC pipe with screen) located in the transition zone, but 1 m away from the soil sampling plot (Supplementary Fig. 1). Plot elevation was determined by use of a Trimble Geo 7× (Trimble Inc., Sunnyvale, CA) and LiDAR. Ambient surface water salinity was determined at each sampling time using a YSI ProDSS (YSI Inc., Yellow Springs, OH, USA).

Sampling occurred during both the wet season (November 2017) and the dry season (March 2018). At each plot, 3 cores were taken to a depth of 30 cm via push-core and field extruded into 3 10-cm intervals for a total of 27 cores. Samples were stored in polyethylene bags on ice and transported to the laboratory, where they remained at 4 °C until the completion of sample analysis. Soil samples were homogenized through mixing and stirring by hand; roots were not removed.

2.2. Soil physicochemical parameters

Following homogenization of each sample, a subsample was dried until constant weight within an oven at 70 °C to determine percent soil moisture. Bulk density was then calculated as dry soil weight per volume for each depth interval. Dried soils were ground (SPEX Sample Prep 8000 M Mixer Mill, Metuchen, NJ) and organic matter content was determined via the loss-on-ignition method. Following ashing at 550 °C for 3 h in a muffle furnace, 50 mL of 1 M HCl was added to each sample. Samples were boiled for 30 min and the digestate was filtered through Whatman #41 filters for colorimetric analysis of total P (Andersen, 1976 with modifications) on an AQ2 Automated Discrete Analyzer (Seal Analytical, Mequon, WI; EPA method 365.1, Rev. 2). Dried, ground subsamples were also used to determine total soil C and N on a Vario Micro Cube CHNS Analyzer (Elementar Americas Inc., Mount Laurel, NJ). Unlike the other biogeochemical parameters, total C, N, P, and organic matter content were only analyzed for the dry season because pilot data indicated these soil nutrient pools did not change seasonally.

Fig. 2. Edges of the transition zone as identified by historical aerial photography. Image on the left shows the leading edge of the transition between saltgrass and cordgrass in 1994, while the left image shows the same zone in 2016. The change in the edge of the transition zone between 1994 and 2016 is roughly 60 m, as estimated through Google Earth. Approximate zone boundaries are highlighted.

2.3. Extractable nutrients and microbial biomass

Within 24 h of sampling, replicate samples of 2.5 g of field-moist soil were weighed into centrifuge tubes. Twenty-five (25) mL of 2 M KCl was added to one set of samples, which were shaken at 125 rpm for 1 h, centrifuged at 5000 rpm for 10 min at 10 °C, and vacuum-filtered through Supor 0.45 μm filters. The filtered sample was acidified to a pH of <2 with double distilled H_2SO_4 and analyzed colorimetrically on an AQ2 Automated Discrete Analyzer for ammonium (NH_4^+), nitrate (NO_3^-), and soluble reactive phosphorus (SRP) (Seal Analytical, Mequon, WI; EPA methods 231-A Rev. 0, 210-A Rev. 1, and 204-A Rev. 0). The second set of samples were fumigated with chloroform for 24 h within a glass desiccator for determination of soil microbial biomass following Vance and others (1987). Samples were then extracted as referenced above. Dissolved organic C (DOC) content was determined for both the initial and fumigated samples via use of a Shimadzu TOC-L Analyzer (Shimadzu Instruments, Kyoto, Japan) and microbial biomass was estimated as the $DOC_{final} - DOC_{initial}$.

2.4. Potential greenhouse gas production and mineralization rates

Seven grams of field-moist soil from each homogenized sample was weighed into glass serum bottles. Bottles were capped with a rubber septa and aluminum crimp, evacuated to −75 mmHg, then purged with 99% O_2-free N_2 gas for 3 h to create an anaerobic environment. Nitrogen-purged artificial seawater matching the surface water salinity at each plot was injected into each bottle to create a slurry (1:2 of soil: water). Each bottle was placed in a dark orbital shaker at 100 rpm and 25 °C. Headspace was collected after 24, 72, 120, 168, and 240 h and analyzed on a GC-2014 gas chromatograph (Shimadzu Instruments, Kyoto, Japan) to determine potential CO_2 and methane production over time. In general, methane peaks were either low or below detection, and thus will not be discussed. To determine the concentration of dissolved inorganic C, soil pH was determined by creating a 1:5 slurry of soil to distilled, deionized water and measured with an Accumet XL200 benchtop pH probe (ThermoFisher Scientific, Waltham, MA, USA). Concentrations of CO_2 were calculated using Henry's Law, the ideal gas law, and a rate determined with linear regression over time ($R^2 > 0.8$; Bridgham and Ye, 2013). Potential CO_2 rates were normalized to grams of dry soil and represent a rate of potential production of CO_2 within an anaerobic environment.

After the 10-day incubation period, 25 mL of 2 M KCl was added to each bottle. Bottles shook for 1 h at 125 rpm and 25 °C, then decanted and vacuum-filtered using Supor 0.45 μm membrane filters. Samples were acidified to a pH of <2 with double distilled H_2SO_4 and analyzed colorimetrically for NH_4^+ and SRP concentrations (Seal Analytical, Mequon, WI; EPA methods 231-A Rev. 0 and 204-A Rev. 0). The potential mineralization rates of both N and P were calculated as the difference in concentration divided by the 10 day incubation period (Roy and White, 2013). As with the potential CO_2 rates, rates of potential N and P mineralization presented here are representative of an anaerobic soil environment.

2.5. Extracellular enzyme activity

Extracellular enzyme activity of *N*-acetyl-β-D-glucosidase (NAG), alkaline phosphatase (AP), β-glucosidase (BG), xylosidase (XY), and cellobiosidase (CB) were determined via fluorometric assays with 4-methylumbelliferyl (MUF)-linked substrates (Table 1). A soil slurry was created by adding 39 mL of distilled, deionized water to 0.5 g of field moist soil. Slurries were shaken on an orbital shaker for 1 h at 25 °C and 125 rpm, then pipetted into clear 96-well plates. Non-limiting MUF-linked substrates specific to each enzyme were added to each sample and measured both initially and after 24 h on a BioTek Synergy HTX (BioTek Instruments Inc., Winooski, VT) at excitation/emission wavelengths of 360/460 nm to determine rates of enzyme activity (Dunn et al., 2014; German et al., 2011).

2.6. Porewater nutrients

Porewater equilibrators (polycarbonate base with evenly spaced 7 mL wells, covered with a 0.45 μm membrane, and driven into the soil to a depth of 35 cm) were assembled in an anaerobic underwater environment prior to deployment (Teasdale et al., 1995). Immediately following soil sample collection, equilibrators were deployed within an undisturbed region of each plot for 10 days. Upon retrieval, cells were extracted using a syringe and 0.45 μm syringe filters, consolidated into 5 cm intervals, and acidified with double distilled H_2SO_4 to a pH of <2. Samples were analyzed for porewater nutrient concentrations (NH_4^+, NO_3^-, SRP, and DOC) as described above.

2.7. Statistical analysis

Statistical analysis was performed in R via RStudio (RStudio Inc., Boston, MA, USA; version 3.4.2). Data were transformed using a logarithmic transformation to meet the assumptions of normality, as determined via the Shapiro-Wilk test. Homogeneity of variance was determined using Levene's test. Initially, a *t*-test was performed to determine whether each parameter was significantly different between seasons; data were then analyzed separately by season.

Data were analyzed via a linear mixed model using package ‘lme4’ (Bates et al., 2015). Model selection was conducted to determine the best linear mixed model based on AICc scores that addressed the experimental hypotheses. All potential models included the random effects of transect and core identity (one level for each individual core), but had varied fixed effects. The four potential models included: y ~ depth, y ~ community, y ~ depth + community, and y ~ depth*community. The best performing model was determined to have the fixed effects of depth and community without including the interaction term. A Bonferroni correction was applied to the initial alpha value of 0.1 due to the number of model iterations, which decreased the alpha value to reject the null hypothesis to 0.0005. Following determination of significance within the linear model, least-square means tests (‘lsmeans’) were applied post-hoc to determine differences among vegetation types (and associated abiotic shifts) and depth intervals, separately.

Cohen's d was used to calculate the effect size of the vegetation change, using the means of each parameter within the end members of the vegetation change. Effect size was also calculated for parameters presented in a companion paper (Steinmuller et al. 2019), where the same biogeochemical properties were analyzed with the same study design along a woody-herbaceous vegetation gradient.

3. Results

3.1. Elevation and salinity

Elevation was 18.4 ± 2.59 cm (NAVD88) within the saltgrass plots, 18.9 ± 3.14 cm within the transition zone, and 51.1 ± 2.52 cm within the cordgrass plots. Dry season surface water salinities were 19.3, 17.7, and 15.2 ppt within the saltgrass, transition, and cordgrass, respectively. This trend was the same during the wet season, though salinities were slightly lower (between 13 and 17 ppt).

3.2. Soil physicochemical properties

During both seasons, soil moisture content was highest in saltgrass plots (71 ± 2.8% and 69 ± 2.2% for the wet and dry seasons, respectively) and lowest in the cordgrass plots (54 ± 4.9% and 52 ± 4.3%, respectively) and always decreased with depth (Table 2). During the wet season, moisture content was positively correlated to extractable NH_4^+ and SRP concentrations, PMN and PMP rates, potential CO_2 production,

Table 1
Enzymes with associated abbreviations, MUF-linked substrates, and function. Data retrieved from ENZYME nomenclature database, ExPASy (Gasteiger et al., 2003).

Enzyme	Abbreviation	MUF-linked Substrate	Enzyme Function
N-Acetyl-β-ᴅ-glucosidase	NAG	4-Methylumbelliferyl *N*-acetyl-β-ᴅ-glucosaminide	Hydrolysis of NAG containing organic compounds
Alkaline phosphatase	AP	4-Methylumbelliferyl phosphate	Hydrolysis of phosphate monesters
β-Glucosidase	BG	4-Methylumbelliferyl β-ᴅ-glucopyranoside	Hydrolysis of organic compounds to liberate glucose
Xylosidase	XY	4-Methylumbelliferyl-β-ᴅ-xylopyranoside	Degradation of xylan within hemicelluloses
Cellobiosidase	CB	4-Methylumbelliferyl β-ᴅ-cellobioside	Hydrolysis of cellulose to release cellbiose

MBC, and all enzyme activity (Supplementary Table 1). Bulk density was also significantly different among vegetation communities during both seasons (Table 2), being highest within the cordgrass plots, and lowest within the saltgrass plots. Bulk density increased with depth and was negatively correlated to all parameters during the wet season (Supplementary Table 1). Total soil C, N, and organic matter content were highest within the saltgrass and transition zone plots and decreased with depth in all plots (Table 2, Supplementary Fig. 1). Total C concentrations ranged from 182 ± 22.4 g kg^{-1} within the saltgrass plots to 110 ± 20.9 g kg^{-1} within the cordgrass plots. Similarly, total N concentrations ranged from 11.3 ± 1.41 g kg^{-1} within the saltgrass plots to 7.29 ± 1.40 g kg^{-1} within the cordgrass plots. Percent organic matter ranged from 38.4 ± 4.44% (saltgrass) to 24.4 ± 4.59% (cordgrass). No statistically significant differences were detected with either vegetation community or depth within the total P data (Table 2, Fig. 3).

3.3. Extractable and porewater nutrients

Extractable NO_3^- concentrations were roughly 70× higher during the dry season, compared to the wet season, and were influenced by vegetation community and depth only during the dry season sampling (Table 2). During the dry season, extractable NO_3^- concentrations decreased from 0 to 10 to 20–30 cm and were higher within the transition and saltgrass plots (18.4 ± 4.87 mg kg^{-1}), compared to cordgrass plots (4.80 ± 0.942 mg kg^{-1}). Dry season extractable NO_3^- concentrations were positively correlated to extractable SRP, PMP rates, potential CO_2 production, MBC, and all enzyme activity (Supplementary Table 1). Extractable NH_4^+ concentrations were negatively correlated to extractable NO_3^- concentrations (Supplementary Table 1).

Extractable NH_4^+ concentrations were roughly 6.6× higher during the wet season, relative to the dry season, but did not differ with vegetation community (Table 2, Fig. 4). Depth did have a significant effect, ranging from 37.7 ± 5.36 mg kg^{-1} at 0–10 cm to 31.2 ± 5.28 mg kg^{-1} at 20–30 cm during the wet season. In contrast, dry season extractable NH_4^+ concentrations averaged 1.62 ± 0.714 mg kg^{-1} at 0–10 cm to 8.92 ± 1.48 mg kg^{-1} at 20–30. Wet season extractable NH_4^+ concentrations were positively correlated to extractable SRP, PMN and PMP rates, potential CO_2 production, MBC, and all enzyme activity (Supplementary Table 1). However, during the dry season, extractable NH_4^+ concentrations were negatively correlated to extractable SRP, PMP rates, MBC, potential CO_2 production, and all enzyme activity.

Concentrations of extractable SRP during the wet season were roughly 18.5× higher than the dry season concentrations. Extractable SRP concentrations differed significantly with vegetation community during the wet season (greater in saltgrass plots, 0.885 ± 0.148 mg kg^{-1}, than cordgrass plots, 0.591 ± 0.105 mg kg^{-1}) and decreased with depth during both seasons (Table 2, Fig. 4). While the wet season extractable SRP concentrations were significantly correlated to PMN and PMP rates, potential CO_2 production, MBC, and all enzyme

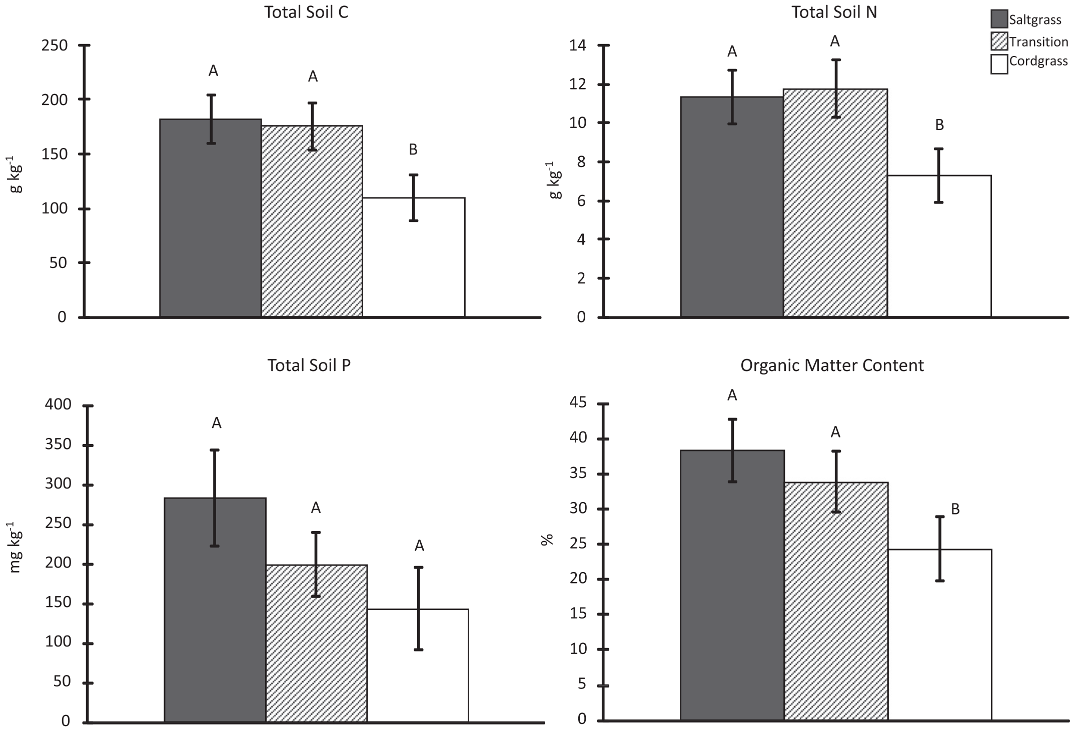

Fig. 3. Total soil carbon, nitrogen, phosphorus, and percent organic matter within each vegetation community. Capital letters denote significant differences between vegetation communities. Statistics were conducted on log transformed data, while plotted data is not log transformed. Data represents mean of all replicates at all soil depths ± standard error.

activity; dry season concentrations were significantly correlated to only PMP rates, MBC, potential CO_2 production, AP activity, BG activity, and AS activity (Supplementary Table 1).

There was no effect of either vegetation community or depth on porewater DOC (both seasons), though the wet season concentrations were approximately 2× more than dry season concentrations. Porewater NH_4^+ increased with depth during the dry season, while porewater SRP increased with depth during both seasons. Porewater SRP was the only porewater nutrient affected by vegetation, with greatest concentrations within the saltgrass zone, followed by the cordgrass zone, then the transition zone during the dry season. However, during the wet season, porewater SRP concentrations were greatest within the cordgrass and lowest within the saltgrass. Porewater NO_3^- values were consistently below detection.

3.4. Microbial biomass and potential CO_2 production

Wet season MBC concentrations were 2.3× higher than MBC concentrations in the dry season, with concentrations ranging from 4998 ± 541 mg kg^{-1} (wet season) and 2354 ± 243 mg kg^{-1} (dry season) within the saltgrass plots, to 3793 ± 632 mg kg^{-1} (wet season) and 1280 ± 249 mg kg^{-1} (dry season) in the cordgrass plots (Tables 2 and 3, Fig. 5). Concentrations of MBC decreased with depth during both seasons and were correlated to potential CO_2 production and all enzyme activity (Supplementary Table 1).

Potential CO_2 production during both seasons decreased with depth (Table 2, Fig. 5), though production rates were 1.4× higher during the wet season. During the wet season, potential CO_2 production within saltgrass plots averaged 2.68 ± 0.626 mg CO_2-C kg^{-1} h^{-1} and cordgrass plots averaged 1.41 ± 0.419 mg CO_2-C kg^{-1} h^{-1} (Tables 2 and 3), but there was no effect during the dry season. Potential CO_2 production was correlated to all enzymatic activity during both seasons (Supplementary Table 1).

3.5. Extracellular enzyme activity and potentially mineralizable N and P rates

All extracellular enzyme activities (AP, NAG, BG, CB, XY, AS) were greater during the wet season than the dry season and decreased with increasing depth (Table 2; Figs. 4, 6). Consistently, enzyme activity was greatest within the saltgrass plots, followed by the transition zone, and lowest within the cordgrass plots. All enzyme activities were significantly correlated to each other during both seasons (Supplementary Table 1).

Table 2
Significance table the linear model testing the additive effects of vegetation community type and depth and random effects of transect and replicate core. Significant *p*-values are denoted by underlined values. Note that no analysis was performed for wet season total soil C, N, P, and organic matter, as indicated by '-'. ($n = 27$ for each season, $\alpha = 0.005$).

	Wet season		Dry season	
	Community	*Depth*	*Community*	*Depth*
Moisture content	<0.0001	<0.0001	<0.0001	<0.0001
Bulk density	<0.0001	<0.0001	<0.0001	<0.0001
Total C	–	–	<0.0001	<0.0001
Total N	–	–	<0.0001	<0.0001
Total P	–	–	0.4147	0.0850
Organic matter	–	–	<0.0001	<0.0001
Extractable NO_3^-	<0.0001	<0.0001	<0.0001	<0.0001
Extractable NH_4^+	0.6787	0.0674	0.0003	<0.0001
Extractable SRP	0.0262	<0.0001	0.0095	<0.0001
Microbial biomass C	0.00029	<0.0001	0.0248	<0.0001
N-acetyl-β-D-glucosidase	<0.0001	<0.0001	0.0001	<0.0001
Alkaline Phosphatase	<0.0001	<0.0001	<0.0001	<0.0001
β-glucosidase	<0.0001	<0.0001	<0.0001	<0.0001
Cellobiosidase	<0.0001	<0.0001	<0.0001	<0.0001
Xylosidase	<0.0001	<0.0001	0.0041	<0.0001
Aryl Sulfatase	<0.0001	<0.0001	<0.0001	<0.0001
Potential CO_2 production	0.0001	<0.0001	<0.0001	<0.0001
Potentially mineralizable N	0.0007	<0.0001	0.2775	<0.0001
Potentially mineralizable P	<0.0001	<0.0001	0.0051	<0.0001

During the dry season, PMN and PMP rates were roughly 2× and 8× higher than during the wet season, respectively (Fig. 4). The saltgrass plots had the highest PMN and PMP rates during both seasons, followed by the transition zone and then the cordgrass plots. Both PMN and PMP decreased with depth.

3.6. Effect size comparisons to mangrove encroachment

Average effect size within the woody-herbaceous transition was 0.7 (Table 3), ranging from 1.8 (Total C) to 0.1 (potential CO_2 rate and BG). The herbaceous-herbaceous transition average effect size of the

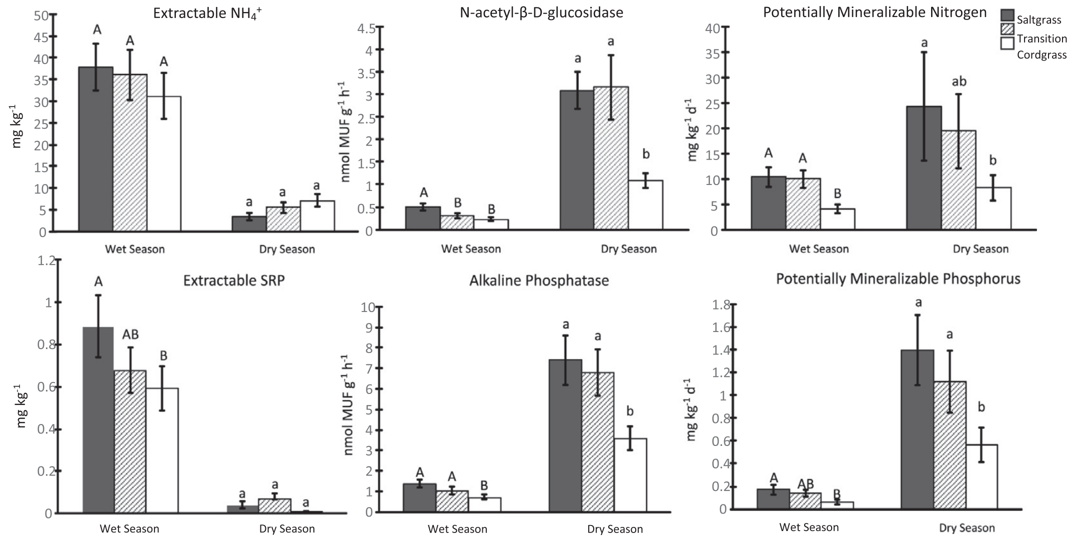

Fig. 4. Soil extractable ammonium, *N*-acetyl-β-D-glucosidase (NAG) activity, potentially mineralizable nitrogen rates, soil extractable soluble reactive phosphorus (SRP) concentrations, alkaline phosphatase activity, and potentially mineralizable phosphorus rates within each vegetation community at both wet and dry seasons. Capital letters denote significant differences between vegetation communities during the wet season, while lowercase letters denote significant differences between vegetation communities during the dry season. Statistics were conducted on log transformed data, while plotted data is not log transformed. Data represents mean of all replicates at all soil depths ± standard error.

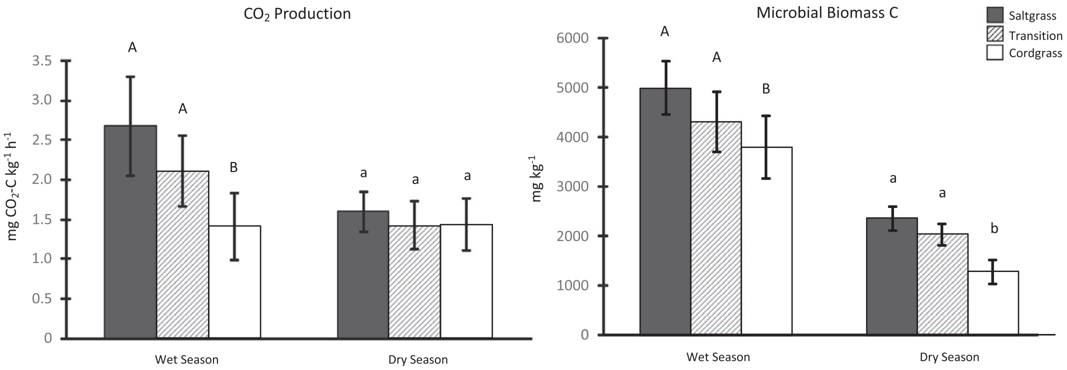

Fig. 5. Soil CO_2 production and microbial biomass carbon concentrations within each vegetation community at both wet and dry seasons. Capital letters denote significant differences between vegetation communities during the wet season, while lowercase letters denote significant differences between vegetation communities during the dry season. Statistics were conducted on log transformed data, while plotted data is not log transformed. Data represents mean of all replicates at all soil depths ± standard error.

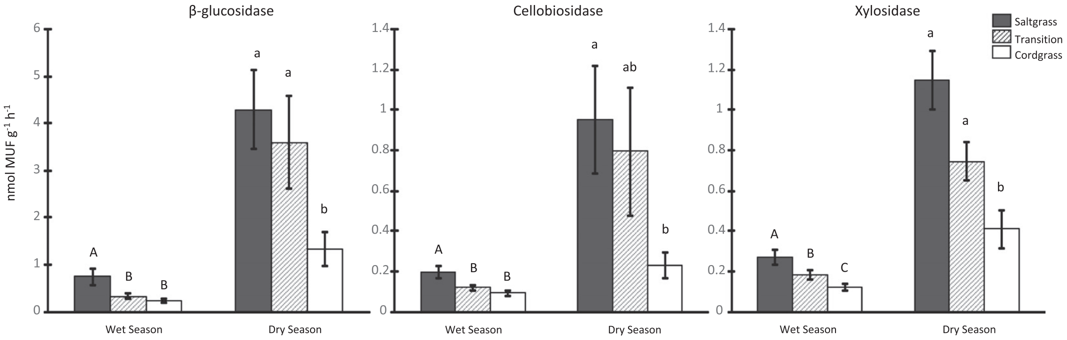

Fig. 6. Activity of soil carbon-degrading enzymes (β-glucosidase, cellobiosidase, and xylosidase) within each vegetation community at both wet and dry seasons. Capital letters denote significant differences between vegetation communities during the wet season, while lowercase letters denote significant differences between vegetation communities during the dry season. Statistics were conducted on log transformed data, while plotted data is not log transformed. Data represents mean of all replicates at all soil depths ± standard error. Supplemental Figure: Weekly average water levels in distance above soil surface (m) and monthly maximum conductivity (mS/cm) recorded from August 2017 to February 2018.

measured parameters was 0.5 (Table 3), ranging from 0.7 (NAG activity) to 0.1 (extractable NH_4^+).

4. Discussion

4.1. Abiotic gradients

The region of marsh dominated by saltgrass coincided with a microtopographical elevation difference of approximately −33 cm, relative to the cordgrass community. This elevation difference contributed to higher surface water salinity and soil moisture content within the saltgrass zones, reflecting a lower position within the tidal range and a greater marine influence. As a result, soils within the saltgrass and transition zones remained saturated during the dry season, while the cordgrass soils experienced dry-down (~20 cm, Supplementary Fig. 1). Although the present experimental design cannot elucidate the causal relationship between vegetation shifts and abiotic gradients, the covariation suggests continued sea level rise will likely favor further encroachment of saltgrass into areas presently dominated by cordgrass. As such, understanding the differences in biogeochemical properties between these two vegetation communities (as well as the accompanying abiotic gradients) is crucial to quantifying potential changes in C, N, and P storage and cycling across the coastal landscape.

4.2. Seasonality

Seasonal differences were likely driven by changes in hydrology; both the seasonal changes in water levels and the greater marine influence acting on the saltgrass and transition zones, due to their lower elevation, likely contributed to observed differences in extractable and porewater nutrient concentrations, speciation of porewater

Table 3
Effect size (Cohen's d) of the vegetation transition (and concomitant abiotic changes) within both the woody-herbaceous transition (data from Steinmuller et al. (2019) and the herbaceous – herbaceous transition (this paper). Effect sizes characterized as trivial (<0.2) are in unshaded cells in italics, small effect sizes (0.2-0.49) are within unshaded cells, medium effect sizes (0.5-0.79) are in shaded in light grey, and large effect sizes (0.8+) are shaded in dark grey.

Parameter	Woody – Herbaceous Transition	Herbaceous - Herbaceous Transition
Total C	1.8	0.6
Total N	1.6	0.5
Total P	0.7	0.4
Organic Matter	1.8	0.6
Extractable NO_3^-	0.6	0.5
Extractable NH_4^+	0.3	*0.1*
Extractable SRP	0.4	0.3
Potentially Mineralizable N Rate	0.7	0.4
Potentially Mineralizable P Rate	0.2	0.5
Microbial Biomass C	0.7	0.4
Potential CO_2 Rate	*0.1*	0.3
N-acetyl-β-D-glucosidase	0.3	0.7
Alkaline Phosphatase	0.6	0.5
β-glucosidase	*0.1*	0.6
Xylosidase	0.6	0.8
Cellobiosidase	0.2	0.5
Average	**0.7**	**0.5**

nitrogen, soil enzyme activity, N and P mineralization, and microbial biomass C content. Increased concentrations of both porewater and extractable SRP, NH_4^+, and DOC during the wet season are likely driven by exchange with the adjacent lagoon (Brockmeyer et al., 1996). The influx of coastal lagoon water could have provided inorganic nutrients and labile C substrates to microbial communities, thereby decreasing enzyme activity and mineralization rates of N and P, relative to the dry season (Figs. 4, 5, 6). Enzyme activity is regulated by microbial need for substrates cleaved from larger organic compounds and, under the evolutionary-economic principle of enzyme activity, it becomes less efficient for microbes to continue production of extracellular enzymes in the presence of the required organic substrates (Allison et al., 2011; Skujiņš and Burns, 1976). Similarly, mineralization rates are regulated by demand for inorganic nutrients and decrease in response to increased availability (Robertson and Groffman, 2007). For example, the abundance of extractable SRP (which includes porewater SRP) during the wet season could have been responsible for the observed decrease in both enzyme activity and P mineralization rates, while low concentrations of SRP within the dry season could support the observed higher enzyme activity and P mineralization rates. This trend was not limited to P; both N and C enzymes exhibited the same relationship (Figs. 4, 5, 6). The availability of inorganic nutrients supplied by the lagoon could also have bolstered microbial biomass C during the wet season by allowing the community to switch from mediating catabolic reactions (such as mineralization) to inputting energy into microbial anabolism and growth (Robertson and Groffman, 2007).

4.3. Soil nutrient storage

Soils within the saltgrass zones stored 37% more total C and 34% more total N than soils within the cordgrass zones, as was hypothesized, which may relate to abiotic factors (e.g., lower elevation) and/or biotic factors (e.g., the unique morphology, productivity rates, and litter quality of the dominant plant species; Fig. 3). The location of the saltgrass zones lower within the tidal frame is expected to limit decomposition by reducing the availability of terminal electron acceptors through the longer and deeper tidal flooding (Sutton-Grier et al., 2011). However, soils within the saltgrass zones supported higher rates of potential CO_2 production and C-degrading enzyme activity than within the cordgrass soils. Both of these measurements imply higher rates of C cycling within the saltgrass zone, which is in opposition to an increase in C storage. This paradox could be an effect of, a) differences in primary production between species (i.e. Choi et al., 2001), b) saltgrass litter being more labile (i.e. lower C:N ratio) than cordgrass litter, or c) an influx of labile DOC from the lagoon supporting higher rates of C turnover within the saltgrass, while still enhancing C storage, or d) abiotic conditions, such as inundation frequency. Regardless of the mechanism facilitating simultaneously higher C storage and C cycling within the saltgrass and transition zone soils, it is evident that encroachment of saltgrass is presently enhancing the burial of both C and N, with implications for landscape-scale C and nutrient budgets.

4.4. Nutrient cycling

Saltgrass zones had greater enzyme activity and mineralization rates than cordgrass zones during both seasons, which was in opposition to our initial hypothesis that the transition zones would function as biogeochemical 'hotspots'. If the combination of water level and nutrient supply from the water column solely controlled enzyme activity and mineralization rates within this system, then the less-inundated cordgrass zones would exhibit the highest enzyme activity and mineralization rates, as low water level facilitates increased breakdown of organic matter and low nutrient availability enhances microbial need for enzymatic cleavage (Allison et al., 2011; McLatchey and Reddy, 1998). Instead, the observed higher rates of enzyme activity and mineralization within the saltgrass soils suggest the presence of a vegetation effect on these processes, such as presence of root exudates, oxidation within the rhizosphere, or differences in root-associated microbiota. In terrestrial systems, soil microbial community structure has been documented to be dependent both on the associated species of vegetation (Berg and Smalla, 2009) and changes in vegetation dominance (Kourtev et al., 2002), suggesting the intrinsic properties of saltgrass and its associated microbiome could account for the increased rates of organic matter processing observed within the saltgrass zones.

Soil NAG, AP, and PMP rates within the transition zone sites were similar to rates expressed by the saltgrass soils, and greater than rates within the cordgrass soils during both seasons. This similarity between the saltgrass and the transition zone indicates that rather than the transition zone functioning as an intermediate as the vegetation community composition would suggest, biogeochemical processing within the transition zone is functionally similar to that of the saltgrass zone. This has important management implications, as it *suggests* altered biogeochemical functioning in an ecosystem prior to the visible shift in plant species, though within this study, we cannot tease apart the biotic influences from abiotic influences. However, these relationships were mediated by season. Specifically, during the dry season BG, CB, and XY, which are indicators of microbial need for cellulose, cellobiose, and xylose, respectively, were similar between the transition and saltgrass zones (Deng and Tabatabai, 1994; Eivazi and Tabatabai, 1988). However, during the wet season, the transition zone soils become more functionally similar to the cordgrass soils in terms of C-degrading enzyme activity, exhibiting a lower need for labile C substrates than the saltgrass. This shift indicates that both season and vegetation type interactively regulate differences in availability and microbial demand for these C substrates between species.

Interestingly, all measured enzyme activity rates within this study were roughly 30–50% lower than observed enzyme activity within a proximal saltmarsh, where saltgrass is being encroached upon by mangrove, rather than acting as the encroaching species (Steinmuller et al. 2019). In contrast, PMN rates in this study were slightly higher than where saltgrass is being encroached upon (Steinmuller et al. 2019). As extractable ammonium concentrations were similar between the two studies, the higher PMN rates observed here could be caused by larger aboveground biomass and/or a greater proportion of fine roots when saltgrass is the encroaching species, rather than the species that is being encroached upon (Ehrenfeld, 2003). These differences in soil biogeochemical processes (i.e. enzyme activity and potential mineralization rates) between encroaching saltgrass and saltgrass experiencing encroachment indicate that, to some extent, the biogeochemical effects of encroachment are dependent on the local ecological context, rather than being universal species-specific responses, similar to trends shown within exotic plant invasions (Ehrenfeld, 2003).

4.5. Comparisons to mangrove encroachment

Many coastal marshes are also experiencing the encroachment of woody species, such as the black mangrove (Armitage et al., 2015; Doughty et al., 2016; Giri et al., 2011; Montagna et al., 2011; Stevens et al., 2006). Steinmuller et al. (2019) reported changes in nutrient cycling along a separate ecological gradient of encroaching black mangroves within a proximal coastal wetland. The combination of these two studies presents a unique opportunity to compare the two vegetation transition types: woody encroaching upon herbaceous vegetation ('woody-herbaceous') and herbaceous encroaching on other herbaceous vegetation ('herbaceous-herbaceous') at sites that are spatially related and face similar drivers (Table 3). Effect size (calculated as Cohen's d) facilitates a comparison of these two sites: larger effect sizes indicate larger implications for ecosystem response to the vegetation transition and abiotic changes.

The average effect size for the both the woody-herbaceous transition and the herbaceous-herbaceous transition were categorized as a 'medium effect' (Cohen, 1988; Table 3). The minimal difference between the effect sizes observed in these two types of transitions may be surprising considering woody species have such dramatically different physiology (Camacho-B et al., 1974; Table 3), metabolic functioning, biomass allocation, and interaction with the edaphic environment than herbaceous species. Moreover, woody encroachment in coastal wetlands has received far more research attention (e.g., 1397 papers between 1998 and 2018) than herbaceous encroachment (357 papers over the same timescale, based on a Web of Science search). Despite the preferential study of mangrove encroachment, this study suggests both types of encroachment (woody-herbaceous and herbaceous-herbaceous) exhibit medium-to-high- effects on biogeochemical properties and processes. Furthermore, mangrove encroachment is geographically confined to predominantly subtropical regions, while herbaceous encroachment is the dominant process throughout temperate coastal wetlands, suggesting the implications of herbaceous-herbaceous coastal marsh encroachment warrants further study.

Further examination of the differences in effect size between the two sites clearly indicates soil nutrient pools with slow turnover rates (total soil C, N, P, and organic matter content) within the woody-herbaceous transition appear to be most affected by encroachment (Table 3). These total nutrient pools provide electron donors to support microbial respiration (Sutton-Grier et al., 2011) and plant growth (Ågren, 2008), contribute to elevation gains through supporting primary productivity (Redfield, 1972), and are responsible for the critical ecosystem services such as sequestration of C. Altering these total soil nutrient pools could quickly disrupt trends in biogeochemical processing and nutrient storage on an ecosystem level. In contrast, the highest effect sizes within the herbaceous-herbaceous transition were observed within the enzyme activities (NAG, AP, BG, XY, and CB), which are indicators of current nutrient availability and lability and reflect soil organic matter pools with shorter residence times. Therefore, as vegetation transitions continue within coastal wetlands, it appears that the largest effects within woody-herbaceous transitions will be to critical stocks of soil nutrients, while short-term pools of labile nutrients cycled by enzymatic activity will be most affected within herbaceous-herbaceous transitions; both results will impact the C storage and ecological functioning of the system as a whole. More studies encompassing different regions and climatic drivers need to be conducted to further understand the effects of both woody-herbaceous and herbaceous-herbaceous encroachment on biogeochemical processing in coastal wetlands, and to disentangle the effects of vegetation encroachment from sea level rise and other abiotic gradients.

5. Conclusions

Biogeochemical functioning is highly dependent on seasonal water levels within this coastal marsh. Both the influx of nutrients and presence of a water column during the wet season generally dampened rates of soil microbial processing of organic matter (enzyme activity and N and P mineralization), while these rates increased during the dry season. The encroachment of saltgrass into this cordgrass-dominated coastal marsh enhanced both total soil nutrient storage and the rate of biogeochemical processing of organic matter. Soil C and N content within the saltgrass marsh was higher than within the cordgrass zones, as were accompanying measures of C loss (i.e. potential CO_2 production) and organic matter processing (i.e. enzyme activity and mineralization of inorganic N and P). Together, these parameters imply that while C storage might increase with saltgrass encroachment, the quantity and quality of C substrates is also increasing, resulting in a concomitant increase in the release of greenhouses gases (i.e., CO_2) and the rate of organic matter turnover.

Leveraging effect size between this study and Steinmuller et al. (2019) demonstrates that though woody-herbaceous encroachment has a larger effect size than herbaceous-herbaceous encroachment, the difference between the two is small. Encroachment has a larger effect on total soil nutrients with a slow turnover time (i.e. total soil nutrients) within the woody-herbaceous site, while at the herbaceous-herbaceous site, short-term biogeochemical indicators (i.e. enzyme activity) were the most affected. While encroachment will continue to alter biogeochemical processing at each site, the woody-herbaceous site is likely to experience slower changes while the herbaceous-herbaceous site will experience rapid disruptions in rates of biogeochemical cycling. More studies investigating the consequences of herbaceous encroachment are critical to understanding both the biogeochemical and ecosystem-level effects of this process on a regional-scale, which can then be leveraged into creating predictions for climate change scenarios using global patterns. As sea level rise accelerates, these vegetation transitions are expected to become more prevalent, further demonstrating the need for characterizing the effects of encroachment.

Supplementary data to this article can be found online at https://doi.org/10.1016/j.scitotenv.2020.139532.

CRediT authorship contribution statement

Havalend E. Steinmuller: Conceptualization; Data curation; Formal analysis; Investigation; Methodology; Writing - original draft; Writing - review & editing**Tammy E. Foster:** Conceptualization; Resources; Writing - review & editing **Paul Boudreau:** Formal analysis; Investigation; Writing - review & editing **C. Ross Hinkle:** Conceptualization; Resources; Supervision; Writing - review & editing **Lisa G. Chambers:** Conceptualization; Data curation; Funding acquisition; Investigation; Methodology; Project administration; Resources; Supervision; Writing - review & editing

Declaration of competing interest

The authors declare that they have no known competing financial interests or personal relationships that could have appeared to influence the work reported in this paper.

Acknowledgements

The authors would like to acknowledge members of the Aquatic Biogeochemistry Laboratory, as well as Lauren Caspers, Russell Lowers, and Dr. Paul Schmalzer for their assistance in the field, as well as Dr. Joshua Breithaupt and Nia R. Hurst for help in the field and insight on improving this manuscript. This project was funded by the University of Central FloridaDepartment of Biology.

References

Ågren, G.I., 2008. Stoichiometry and nutrition of plant growth in natural communities. Annu. Rev. Ecol. Evol. Syst. 39, 153–170. https://doi.org/10.1146/annurev.ecolsys.39.110707.173515.

Allison, S.D., Weintraub, M.N., Gartner, T.B., Waldrop, M.P., 2011. Evolutionary-economic principles as regulators of soil enzyme production and ecosystem function. In: Shukla, G., Varma, A. (Eds.), Soil Enzymology. Springer Berlin Heidelberg, Berlin, Heidelberg, pp. 229–243. https://doi.org/10.1007/978-3-642-14225-3_12.

Andersen, J.M., 1976. An ignition method for determination of total phosphorus in lake sediments. Water Res. 10, 329–331. https://doi.org/10.1016/0043-1354(76)90175-5.

Armitage, A.R., Highfield, W.E., Brody, S.D., Louchouarn, P., 2015. The contribution of mangrove expansion to salt marsh loss on the Texas Gulf Coast. PLoS One 10, e0125404.

Bates, D., Mächler, M., Bolker, B., Walker, S., 2015. Fitting linear mixed-effects models using lme4. J. Stat. Software 1 (1). https://doi.org/10.18637/jss.v067.i01.

Berg, G., Smalla, K., 2009. Plant species and soil type cooperatively shape the structure and function of microbial communities in the rhizosphere. FEMS Microbiol. Ecol. 68, 1–13. https://doi.org/10.1111/j.1574-6941.2009.00654.x.

Bertness, M.D., 1991. Zonation of Spartina Patens and Spartina Alterniflora in New England Salt Marsh. Ecology 72, 138–148. https://doi.org/10.2307/1938909.

Bridgham, S.D., Ye, R., 2013. Organic matter mineralization and decomposition. Methods Biogeochem. Wetl. 385–406.

Brockmeyer, R.E., Rey, J.R., Virnstein, R.W., Gilmore, R.G., Earnest, L., 1996. Rehabilitation of impounded estuarine wetlands by hydrologic reconnection to the Indian River lagoon, Florida (USA). Wetl. Ecol. Manag. 4, 93–109. https://doi.org/10.1007/BF01876231.

Camacho-B, S.E., Hall, A.E., Kaufmann, M.R., 1974. Efficiency and regulation of water transport in some woody and herbaceous species. Plant Physiol. 54, 169 LP–172.

Choi, Y., Hsieh, Y., Wang, Y., 2001. Vegetation succession and carbon sequestration in a coastal wetland in northwest Florida: evidence from carbon isotopes dominated by duncus which is a C3 plant and has an average lesser amounts of other species, are also present in the area. The b • 3C. Glob. Biogeochem. Cycles 15, 311–319.

Cohen, J., 1988. Statistical Power Analysis for the Behavioural Sciences.

Darrouzet-Nardi, A., D'Antonio, C.M., Dawson, T.E., 2006. Depth of water acquisition by invading shrubs and resident herbs in a Sierra Nevada meadow. Plant Soil 285, 31–43.

Deng, S.P., Tabatabai, M.A., 1994. Cellulase activity of soils. Soil Biol. Biochem. 26, 1347–1354.

Doughty, C.L., Langley, J.A., Walker, W.S., Feller, I.C., Schaub, R., Chapman, S.K., 2016. Mangrove range expansion rapidly increases coastal wetland carbon storage. Estuar. Coasts 39, 385–396. https://doi.org/10.1007/s12237-015-9993-8.

Dunn, C., Jones, T.G., Girard, A., Freeman, C., 2014. Methodologies for extracellular enzyme assays from wetland soils. Wetlands 34, 9–17. https://doi.org/10.1007/s13157-013-0475-0.

Ehrenfeld, J.G., 2003. Effects of exotic plant invasions on soil nutrient cycling processes. Ecosystems 6, 503–523. https://doi.org/10.1007/s10021-002-0151-3.

Eivazi, F., Tabatabai, M.A., 1988. Glucosidases and galactosidases in soils. Soil Biol. Biochem. 20, 601–606.

Foster, T.E., Stolen, E.D., Hall, C.R., Schaub, R., Duncan, B.W., Hunt, D.K., Drese, J.H., 2017. Modeling vegetation community responses to sea-level rise on Barrier Island systems: a case study on the Cape Canaveral Barrier Island complex, Florida, USA. PLoS One 12, 1–22. https://doi.org/10.1371/journal.pone.0182605.

Gasteiger, E., Gattiker, A., Hoogland, C., Ivanyi, I., Appel, R.D., Bairoch, A., 2003. ExPASy: the proteomics server for in-depth protein knowledge and analysis. Nucleic Acids Res. 31, 3784–3788. https://doi.org/10.1093/nar/gkg563.

German, D.P., Weintraub, M.N., Grandy, A.S., Lauber, C.L., Rinkes, Z.L., Allison, S.D., 2011. Optimization of hydrolytic and oxidative enzyme methods for ecosystem studies. Soil Biol. Biochem. 43, 1387–1397. https://doi.org/10.1016/j.soilbio.2011.03.017.

Giri, C., Ochieng, E., Tieszen, L.L., Zhu, Z., Singh, A., Loveland, T., Masek, J., Duke, N., 2011. Status and distribution of mangrove forests of the world using earth observation satellite data. Glob. Ecol. Biogeogr. 20, 154–159.

Knapp, A.K., Briggs, J.M., Collins, S.L., Archer, S.R., BRET-HARTE, M.S., Ewers, B.E., Peters, D.P., Young, D.R., Shaver, G.R., Pendall, E., 2008. Shrub encroachment in North American grasslands: shifts in growth form dominance rapidly alters control of ecosystem carbon inputs. Glob. Chang. Biol. 14, 615–623.

Koch, G.W., Mooney, H.A., 1996. Response of terrestrial ecosystems to elevated CO2: a synthesis and summary. Carbon dioxide Terr. Ecosyst. 415.

Kourtev, P.S., Ehrenfeld, J.G., Häggblom, M., 2002. Exotic plant species alter the microbial community structure and function in the soil. Ecology 83, 3152–3166. https://doi.org/10.1890/0012-9658(2002)083[3152:EPSATM]2.0.CO;2.

Liao, Chengzhang, et al., 2008. "Altered ecosystem carbon and nitrogen cycles by plant invasion: a meta-analysis.". New phytologist 177 (3), 706–714 APA.

McLatchey, G.P., Reddy, K.R., 1998. Regulation of organic matter decomposition and nutrient release in a wetland soil. J. Environmenal Qual. https://doi.org/10.2134/jeq1998.00472425002700050036x.

Montagna, P.A., Brenner, J., Gibeaut, J., Morehead, S., 2011. Coastal Impacts. Impact Glob. Warm. Texas. pp. 96–123.

Osland, M.J., Enwright, N.M., Day, R.H., Gabler, C.A., Stagg, C.L., Grace, J.B., 2016. Beyond just sea-level rise: considering macroclimatic drivers within coastal wetland vulnerability assessments to climate change. Glob. Chang. Biol. 22, 1–11. https://doi.org/10.1111/gcb.13084.

Ouyang, X., Lee, S.Y., 2014. Updated estimates of carbon accumulation rates in coastal marsh sediments. Biogeosciences 11, 5057–5071. https://doi.org/10.5194/bg-11-5057-2014.

Pennings, S.C., Callaway, R.M., 1992. Salt Marsh Plant zonation: the relative importance of competition and physical factors. Ecology 73, 681–690.

Pennings, S.C., Grant, M.-B., Bertness, M.D., 2004. Plant zonation in low-latitude salt marshes: disentangling the roles of flooding, salinity and competition. J. Ecol. 93, 159–167. https://doi.org/10.1111/j.1365-2745.2004.00959.x.

Ratajczak, Z., Nippert, J.B., Collins, S.L., 2012. Woody encroachment decreases diversity across north American grasslands and savannas. Ecology 93, 697–703. https://doi.org/10.1890/11-1199.1.

Redfield, A.C., 1972. Development of a New England salt marsh. Ecol. Monogr. 42, 201–237. https://doi.org/10.2307/1942263.

Robertson, G.P., Groffman, P.M., 2007. Nitrogen transformations. Soil Microbiology, Ecology and Biochemistry, Third edition Elsevier, pp. 341–364.

Roy, E.D., White, J.R., 2013. Measurements of nitrogen mineralization potential in wetland soils. Methods in Biogeochemistry of Wetlands. SSSA Book Series SV - 10. Soil Science Society of America, Madison, WI, pp. 465–471 https://doi.org/10.2136/sssabookser10.c24.

Skujiņš, J., Burns, R.G., 1976. Extracellular enzymes in soil. CRC Crit. Rev. Microbiol. 4, 383–421.

Stevens, P.W., Fox, S.L., Montague, C.L., 2006. The interplay between mangroves and saltmarshes at the transition between temperate and subtropical climate in Florida. Wetl. Ecol. Manag. 14, 435–444.

Steward, Joel S., et al., 2003. "Indian River Lagoon surface water improvement and management (SWIM) plan, 2002 update.".

Sutton-Grier, A.E., Keller, J.K., Koch, R., Gilmour, C., Megonigal, J.P., 2011. Electron donors and acceptors influence anaerobic soil organic matter mineralization in tidal marshes. Soil Biol. Biochem. 43, 1576–1583. https://doi.org/10.1016/j.soilbio.2011.04.008.

Steinmuller, Havalend E., et al., 2019. "Tipping Points in the Mangrove March: Characterization of Biogeochemical Cycling Along the Mangrove–Salt Marsh Ecotone.". Ecosystems 1–18.

Teasdale, P., Batley, G., Apte, S., Webster, I., 1995. Pore water sampling with sediment peepers. TrAC Trends Anal. Chem. 14, 250–256. https://doi.org/10.1016/0165-9936(95)91617-2.

Vance, Eric D., Brookes, Peter C., Jenkinson, David S., 1987. "An extraction method for measuring soil microbial biomass C.". Soil biology and Biochemistry 19.6, 703–707.

Vitousek, P.M., Mooney, H.A., Lubchenco, J., Melillo, J.M., 1997. Human domination of earth' s ecosystems. Science 277, 494 LP–499 (80-.).